Smart Agricultural Technology 5 (2023) 100306

Contents lists available at ScienceDirect

Smart Agricultural Technology

journal homepage: www.journals.elsevier.com/smart-agricultural-technology

A new computer vision workflow to assess yield quality traits in bush bean (*Phaseolus vulgaris L.*)

D. Jollet [a,*], L.V. Junker-Frohn [a], A. Steier [a], T. Meyer-Lüpken [b], M. Müller-Linow [a]

[a] Institute of Plant Sciences, Forschungszentrum Jülich GmbH, Jülich, Germany
[b] Van Waveren Saaten GmbH, Rosdorf, Germany

ARTICLE INFO

Keywords:
Horticultural crop grading
Plant breeding
RGB imaging
Mask R-CNN
Random forest classifier
High-throughput
Digital phenotyping

ABSTRACT

Quality assessments of horticultural products are still often carried out manually in breeding contexts, although computer vision systems have been reported to be able to overcome the limitations of manual assessments, e.g. in automated food processing. Here, a new computer vision workflow for quality trait assessment of bush bean pods (*Phaseolus vulgaris*) is introduced to replace physical measurements and visual scorings of expert breeders, while increasing consistency, accuracy, and objectivity of the measurements. A closed imaging box was used to take images of bean pods from 40 different varieties to develop and validate computer vision workflows to assess breeding relevant shape and color traits of bean pods. For the detection of beaks and peduncles via a neural network approach (Mask R-CNN) accuracies of 95.5% were reached. Computer vision estimations and manual reference measurements of length and caliber were highly correlated (R=0.99). Also, curvature and brightness of green bean pods well- correlated with visual scorings of expert breeders (R=0.81, R=-0.87). A Random Forest Classifier was trained to distinguish yellow and extremely rare bicolored pods and a cross validation accuracy of 83 ±7% was reached. An additional backlight LED panel enabled non-destructive analysis of seed formation inside the pod and promising results were achieved using a Faster R-CNN model. This new computer vision workflow provides the opportunity to replace well-established manual workflows for quality trait assessment of bush bean pods as it is more objective, reliable, and considerably faster.

1. Introduction

Bush bean (*Phaseolus vulgaris L.*) is the most important legume worldwide and provides essential nutrients such as proteins, calories, dietary fibers, B-complex vitamins, and minerals for the diet of a large part of the world's population [1,2]. Bush bean breeding programs not only focus on parameters such as yield and nutrient content, but also on stress tolerance, industrial processability and the visual appearance of the bean pods, which affect the market value. The market value of bush bean is generally determined by yield quality traits related to the bean pod shape like length, caliber, and curvature and also by the color impression [3–5]. Other properties that determine the pod shape and also affect mouthfeel during eating are related to the number and size of seeds inside the pod and the seed arrangement [3]. In addition to the above attributes, it is desirable, for mechanical harvesting, to breed varieties which can be gathered without the peduncle to ease further processing [6].

For many crops, including beans, evaluation of fruit quality traits is performed through visual assessments and manual measurements. This approach is labor-intensive and requires skilled raters, making it the bottle neck in today's breeding programs [7]. Some traits, such as the arrangement of seeds within pods, are scored non-destructively. Therefor they are evaluated indirectly, e.g. by tactile sensing of the outer shape of the pod. In addition, visual scoring of traits is subject to the individual perception of the rater and can additionally be affected by environmental conditions, such as lighting quality and interference by ambient lighting. Consequently, scores of different raters can vary distinctly and even the results of each rater may show noticeable day-by-day variations [8,9]. Manual measurements may be subject to deviations as well, e.g. as a result of individual implementations within established protocols. To overcome this bottleneck, novel approaches are required that are reliable, objective and fast [9,10] and therefore also make sense from an economical point of view [11].

In recent years, a lot of effort has been put into the development and application of various imaging methodologies for horticultural crop phenotyping, including spectral [12,13], thermal [14,15], or 3D

* Corresponding author.
E-mail address: dirk.jollet@kws.com (D. Jollet).

https://doi.org/10.1016/j.atech.2023.100306
Received 30 December 2022; Received in revised form 18 August 2023; Accepted 20 August 2023
Available online 21 August 2023

imaging [16]. The majority of studies used RGB (Red-Green-Blue) imaging, e.g. to assess the shoot and root morphology of carrots [17], or to determine the size of banana fruits [18]. Advantages of RGB imaging systems are that they are low cost, rapid image acquisition, high resolution, and relatively easy implementation [19,7].

However, image analysis can be a complex task and, to date, computer vision methods have been developed only for a small range of vegetable crops. Fruit detection methods have been used to predict the yield and are also a prerequisite for the development of automatic harvest methods [20]. A common use-case are tomatoes. Red mature tomato fruits were detected on greenhouse-grown plants using conventional image processing approaches like the segmentation in the Hue-Saturation-Value (HSV) color space and morphological transformations [21]. Machine learning approaches like X-mean clustering and Random Forest Classification (RFCs) have been successfully applied in the detection of mature, immature, and young tomato fruits of greenhouse-grown plants [22]. In recent years, deep learning approaches offered new opportunities to process complex, high-level abstract and heterogeneous images [23]. Mask region-based convolutional neural networks (Mask R-CNNs) were applied for instance segmentation tasks, i.e. to detect, classify and mask objects in images [24]. This approach was used to detect green and red tomato fruits in images of tomato plants, which were acquired under changing illumination conditions in an experimental greenhouse setup with a set of standard RGB cameras [25].

Only a few studies focused on quality traits of the harvested fruits. Contour-based features of cut tomato fruits were assessed with a contour feature extraction method [26]. A similar approach was used by Torres et al. (2012) and Polder et al. (2012), who quantitatively measured different shape traits like length, area, or beak area of green bean pods [4,27]. Another approach that features different machine learning techniques helped to analyze maize cops and their kernels [29]. In this study, a Fast Fourier Transform was applied to measure the average space each kernel occupies along the cob axis, while the kernel contour was analyzed with a Bayesian approach to identify the beak [28]. In another work, RFC of contour features of bean pods was applied to identify beaks and peduncles. However, finding the correct cutting point to remove these complex and non-uniform structures for further analysis was still error prone [29]. Another study classified green coffee beans by subtle differences in color using neural networks and Bayesian classifier [30].

In this study, we present a number of new validated methods to analyze various shape and chromatic traits of bean pods using a combination of conventional image processing, machine and deep learning. Our approach robustly identifies beaks and peduncles and masks them for further analysis of length, caliber and curvature. In addition, the number of detected peduncles and beaks provides information about the industrial processability. We also developed a new method to quantify chromatic bean pod traits which reflect typical properties of the breeders' scoring scheme like hue and brightness. The quality of assessment of shape and color traits was validated using a dataset of 40 varieties with 400 bean pods in total (green and yellow bean pods with different cross-sectional profiles) that were scored physically by breeding experts in tandem with our computer vision workflow. In the last part, a novel imaging setup using backlight combined with deep learning analysis was developed to characterize the uniformity of the pod's seed arrangement. This is to our knowledge the first method to automatize the analysis of seeds inside the pod. The method was validated with a dataset of 117 bean pods of two contrasting varieties.

2. Methods and materials

2.1. Plant material

The computer vision workflow for peduncle and beak classification and analysis of pod length, caliber, curvature, hue, and brightness of green pods was developed and validated with separate data sets, each including 40 varieties of bush beans (*Phaseolus vulgaris* L.) provided by *van Waaveren Saaten GmbH* (Rosdorf, Germany). Among the selected cultivars were 31 green and 9 yellow varieties, with some of the yellow varieties having an unwanted tendency towards greenish discoloration of bean pods (bicolor). Among the green and yellow cultivars, three categories were distinguished according to their cross-sectional shape, namely *Round* bean pods with a circular cross-section, *Flat* bean pods with a highly ellipsoid cross-section and *Oval* bean pods with an intermediate shape [5]. The varieties showed a wide variation in average pod length, caliber, and curvature, also between individual bean pods Plants were grown according to standard practice at a breeder's field site (Rosdorf, Germany) in summer 2021. The field (51.505332, 9.880956) was treated with 500kg/ha calcium cyanamide on April 10 to fertilize the soil and to antagonize larvae of the bean seed fly (*Delia platura*). Furthermore, an herbicide treatment with 0.5l/ha *Spectrum*® (*BASF*, Ludwigshafen, Germany) + 0.15l/ha *Centium 36CS* (*FMC Agricultural Solutions,* Philadelphia, USA) was conducted four days before sowing. Sowing was conducted on May 14 with an intra and inter row spacing of 8cm and 75cm, respectively. To reduce herbivores, plants were treated with 0.25kg/ha *Pirimor* (*Syngenta Agro GmbH,* Frankfurt, Germany) granulate, and 0.075l/ha *Karate Zeon* (*Syngenta Agro GmbH,* Frankfurt, Germany) on July 21. On July 27 and 28, at BBCH 75-79, fresh maturity (green-ripe) plants were harvested by hand. 780 bean pods from 40 varieties (15-20 pods per variety) were selected so that each group included pods with and without peduncles.

For the analysis of seed arrangement, ten plants of both a green and yellow variety were seeded in 3l pots on ED73 substrate (*Einheitserde Werkverband e.V.,* Uetersen, Germany) on September 13, 2021 and grown under semi-controlled conditions in the greenhouse. Temperature was adjusted to 25/18°C (day/night), relative humidity to 50% and supplemental lighting with MGR-K 400 lamps (*DH Licht GmbH,* Wülfrath, Germany) to a 16/8h day/night cycle. The two varieties were harvested at different maturity stages to assess the robustness of our method. In the green variety, 107 bean pods were harvested on October 28 at very early fresh maturity (BBCH 75-76), so the seeds were relatively small. In the yellow variety, 220 pods were harvested on November 10 (BBCH 79). In this case, the maximum seed size was reached.

2.2. Visual scorings and physical measurements

Experienced bean breeders manually and visually assessed bean pod traits according to their standard practice to gather reference data for the CV algorithm validation. The used standard practices differ from phenotypic bean pod characterization according to UPOV (International Union for the Protection of New Varieties of Plants) guidelines for some traits, as the used scales allow a more subtle evaluation of the pods. Nevertheless, a pod characterization of all used varieties according to UPOV guidelines was added (supplement 1) for better comparison to other studies. It was recorded, if the bean pod had a peduncle and a beak. Pod length was measured as the distance between beak and peduncle base with a ruler by unbending the pod as far as possible without breaking it. The caliber was measured with a circle drawing template (0.5 mm resolution). The curvature, hue, and brightness (only for green bean pods) were assessed visually. Bean pod curvature was assessed on a scoring from 1, straight, to 9, highly curved (more than crescent). As straight bean pods are favored in breeding programs [6], the visual scale distinguishes pods with low curvature (scoring class 1-4) more subtly than cases with higher curvature (5-9). Green bean pod varieties are bred to be moderate green to dark green [6]. The brightness impression of green-colored pods (green brightness) was also scored visually with numbers between 1 (whitish bean pod) to 9 (dark green pod). For yellow bean pods, brightness is irrelevant for consumer decisions, but any greenish discolorations are unwanted, as they are perceived as low-quality. Such bean pods were classified as bicolor.

Breeders usually assess seed numbers and further properties of the seed arrangement by evaluating the outlining of the individual seed bulging. As this turned out to be erroneous, it was scored visually on the transmitted light images. Gaps between two seeds or between the beak and a seed were assigned to the class of abortions and usually occur, if seeds have not been formed. Missing seeds in the upper fourth of the proximal end of the pod are referred to as swan necks.

2.3. Hardware setup and imaging workflow

A customized imaging box with stucco surface reflective walls was used for imaging the bean pods. The top of the imaging box was completely covered by a LED panel with integrated camera opening in the center (*Effilux,* Huerth, Germany). The panel was used with an illuminance of 40000lx (at 0cm distance). The base plate covered an area of 50 × 38 cm and consisted of a robust blue polypropylene plate (*Item*, Solingen, Germany), whose color and low reflectance properties facilitated the pod detection. The distance between camera lens and target area was 80cm. Images were acquired with an industrial RGB camera *Manta G-507* (*Allied Vision,* Stadtroda, Germany, 5MP) equipped with a 12mm FL-CC1218-5MX lens (*Ricoh,* Rungis*, France*). The pixel-metric was converted to the mm-metric according to a calibration method, introduced in Zhang (1998) [31]. At the same time, we checked for considerable radial distortions, which were not observed at 80cm imaging distance (see also [29]). The camera was operated via the *Vimba Viewer 5.1* Software (*Allied Vision,* Stadtroda, Germany). The exposure time was set to 1.4ms with a gain of 0 and a gamma-value of 1. The white balance was performed with the color calibration target *ColorChecker Passport Photo 2* (*Xrite,* Planegg-Martinsried, Germany); values of 2.4 and 2.0 were fixed for the red and the blue channel. The *ColorChecker* was further used to validate that no changes in illumination occured during the 16h of system runtime. Bean pods were placed in the imaging box right after the visual inspection by the expert breeder. One image per variety each with 10 bean pods was acquired (Fig. 1a). Bean pods were arranged on the base plate from left to right in order of the reference measurements (see Fig. 1b). It was paid attention that bean pods did not touch each other or exceed the borders of the blue base plate.

The same box, but equipped with an LED backlight panel, was used to facilitate the detection of seeds, abortions and swan necks in bean pods by highlighting seeds due to their lower transmittance. For this mode, a *LEDP260C* LED backlight panel (*GODOX Photo Equipment Co. Ltd,* Shenzhen, China) was mounted on the base plate, while the top LED panel was turned off. The light intensity of the backlight LED was adjusted to optimize the contrast between seeds and pod. Images of green bean pods were acquired with an illuminance of 14000lx and an exposure time of 8ms. Yellow bean pods, which are more translucent, were imaged with an illuminance of 4000lx (measured at 0cm) and an exposure time of 15ms. For each variety, 6 images of a set of 10 bean pods (in some cases only 9 depending on the availability) were acquired, as this was the maximum number of bean pods that fit on the LED backlight.

2.4. Image processing and digital scoring

2.4.1. Frame conditions and image pre-processing

Image processing tools were developed with *Python 3.9* [32] using *Numpy 1.20.2* [33], *OpenCV 4.5.1.48* [34], *scikit-learn 1.0.1* [35] libraries, and the *Detectron2* [36] framework from *Meta AI* (formerly: *Facebook AI, Menlo Park, USA*). The development of computer vision (CV) methods for curvature and green brightness as well as neural network training (mask R-CNN) for beak and peduncle detection and localization was realized using 380 images of single bean pods. The validation was based on 400 images. For the characterization of the seed arrangement, a neural network was trained with 210 backlight images (160 of yellow and 50 of green pods). The prediction was conducted with a separate image set of 57 green pods and 60 yellow pods. Before analysis, RGB images were pre-processed as follows: For a robust pod segmentation, everything outside the blue background as well as the ColorChecker (containing green patches) was masked out (Fig. 1b). Illumination gradients at the bottom of the imaging box were corrected with a 2D Gaussian distribution function. Furthermore, the RGB image was converted to the Hue-Saturation-Value (HSV) color space. Pixels that belonged to bean pods were separated from background pixels by thresholding the hue channel (*OpenCV* value range: 0-179) with values below a predefined threshold, in our case 80. Next, the image was automatically split up into image sections each containing a single complete bean pod that was analyzed as follows.

2.4.2. Detection of peduncles and beaks

To find and classify peduncles and beaks of the pods and mask them for further analysis, a *mask region based convolutional neural network* (*Mask R-CNN*) from the *Detectron2* framework was employed (pre-trained with ImageNet data from *Detectron2*; Model Zoo[1] [37]), with a *Feature Pyramid Backbone Network,* a *ResNet* backbone of 101 layers and a 3x learning rate schedule. For the training, the *beak* and *peduncle* classes were annotated in 380 images each with a single bean pod using the *VGG Image Annotator* [38]. The dataset was split into 295 training and 85 validation images resulting in a training data set of 293 labeled beaks and 164 peduncles, and a validation data set of 83 labeled beaks and 47 peduncles. The default setting (from Detectron2) of training hyperparameters was used except for the batch size per image and the base learning rate that were adjusted to 256 and 0.00025, respectively. The evaluation with the validation dataset was conducted every 1000 epochs using a continuous increase of the validation loss (3 times) as stop criterion. The training stopped after 35000 epochs. For augmentation, the shortest edge was resized to 100 pixels keeping the aspect ratio of the images unchanged to get a standardizedinput for the network. Images were randomly flipped and rotated between 1-360 degrees to simulate all kind of possible bean pod orientations. Saturation, brightness and contrast were randomly adjusted between 0.75 and 1.25. For inference, the weights at the validation stop were used with a confidence threshold of 0.5. The class predictions were used to estimate the percentage of pods with peduncles and to compute the masks to delete peduncles and beaks in the images for further analysis.

2.4.3. Length, caliber, and curvature

A binary mask was computed from each detected pod (beaks and peduncles excluded). A center line, which corresponds to the pod length, was obtained by computing the topological skeleton and refining the results with iterative pruning (details are given in [29]). The pod length was then estimated by calculating the length of the center line (Fig. 1b) with the *arclength* function (*OpenCV*). The caliber was estimated by finding the maximum width of the mask along the pod's center line. For this purpose, mask widths were measured orthogonally at any position of the center line by applying local linear fits on the surrounding 40 center line pixels [29]. The estimate of pod curvature was also based on the center line position. A cartesian coordinate system was aligned to the center line, such that the line was maximally stretched along the x-axis. As a result, only one y-value per x-axis position is given except for rare cases of extremely crooked pods. A fifth-degree polynomial function was fit to the center line, whose second derivative represents the curvature at any point. To match the breeder's visual assessment, which is more affected by a curved pod center than crooked ends, the curvature function was multiplied by a double symmetrical sigmoid function with values between 0 for the pods' ends and 1 for the center region (see supplement 2). The total pod curvature was calculated as the mean of all measured curvatures along the center line.

[1] Model ID: 138205316 https://github.com/facebookresearch/detectron2/blob/main/configs/COCO-InstanceSegmentation/mask_rcnn_R_101_FPN_3x.yaml

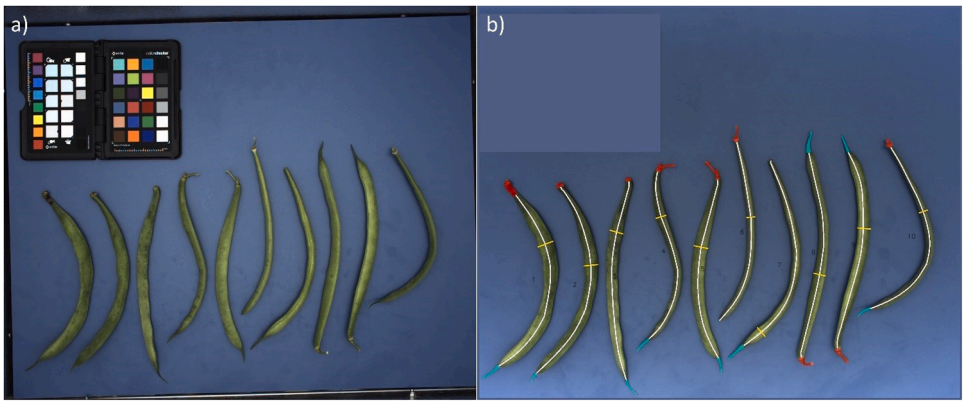

Fig. 1. Image of ten bean pods before (a) and after (b) processing. (b) Mask R-CNN predictions for peduncles (red) and beaks (cyan); the white lines indicate the pod's: center line used for computation of length, and curvature; the yellow lines indicate the positions of caliber measurement.

2.4.4. Seed arrangement

RGB images acquired with LED backlight were analyzed with respect to the seed number and the presence of abortions and swan necks. Images were processed as described before (see 2.4.1) to obtain image sections of single bean pods. To reduce the image content to the essential information, all images were transformed to grayscale. For the object detection task, a *Faster R-CNN* (with model features and pre-training[2] as described for the Mask R-CNN in section 2.4.2) was selected. In total, 210 images (see 2.1) of single bean pods were labeled with the *VGG Image Annotator* [38] according to the three classes: seeds, abortions, and swan necks. The dataset was split into 170 training and 40 validation images. The training data contained 713 labeled seeds, 90 abortions, and 75 swan necks. The validation data contained 160 labeled seeds, 22 abortions, and 15 swan necks. Hyperparameters for training, image augmentation and the stop criterion were set as described in section 2.4.2. The training stopped after approximately 15000 epochs. The confidence threshold for model predictions was set to 0.5.

2.4.5. Chromatic traits

The two chromatic traits hue and green brightness were analyzed using the HSV color space, as it represents particular aspects of the breeders' scoring practice, which comprises the two scales hue and brightness, as well [39]. The HSV values of the masked bean image were analyzed in a two-stage process. In the first step, the hue channel was used to separate green bean pods from yellow and bicolor bean pods. The percentage of pixels which were green (hue: 35-80) and yellow (hue: 15-35) was calculated. Color boundaries were set according to hue space definition in [40]. After applying a majority decision, the 90 pods that were identified as non-green were analyzed in the second step with a RFC model to distinguish between yellow and bicolored pods. The RFC model was trained using 10 features: the percentage and the mean hue values of green and yellow pixels, and the mean and standard deviation of hue, saturation and value of all pod pixels. Data were randomly split in 72 training and 18 validation images of single bean pods. The RFC model was parametrized as follows (see *scikit-learn* function *RandomForestClassifier* for details*): number* of decision trees 100; *quality criterion* '*entropy*', which controls the split at each node in the tree, affecting the overall tree structure. All other parameters were left unchanged to the default settings. In the second step for the pods classified as green, brightness was computed from the mean of the value channel. To avoid the biasing effect of shade gradients at the pods' rounded edges, each mask was eroded by 15 pixels.

[2] Model ID: 137851257 https://github.com/facebookresearch/detectron2/blob/main/configs/COCO-Detection/faster_rcnn_R_101_FPN_3x.yaml

2.5. Statistical tools for method validation

The detection of peduncles, beaks, seeds, swan necks, abortions, and the hue classification was judged by calculating recall, precision and accuracy from confusion matrices, which relate the computer vision results to the reference measurements. The detection of seeds and abortions was summed up in one statistic (confusion matrix).Separate analyses for the numbers of seeds and abortions per pod are presented insupplement 3. In addition, the localization accuracy of the Mask R-CNN for beaks and peduncles was estimated with the mAP50, which describes the mean average precision among all classes at an intersection over union of at least 50% between the labeled and predicted mask. For the traits length, caliber, curvature and green brightness the agreement between reference and computer vision data was examined using regression statistics. Linear regressions were computed using *polyfit* (numpy). The mean absolute percentage error (MAPE) and the correlation coefficient I were used as indicators of the performance of the method. Outliers were identified visually and a residual analysis was conducted to show that the CV methods cover the characteristics of different bean pod categories *Round, Oval*, and *Flat*. When statistically significant differences between the defined categories were observed via One-Way Analysis of Variance (ANOVA) effect size computation (Cohen's D) was additionally conducted. The effect size D measures the standardized difference between two means and is categorized as follows: small <0.5, medium 0.5-0.8, large >0.8 [41]. For the classification of yellow and bicolor pods, a cross validation was conducted (due to the limited number of bicolored bean pods) with 10 subgroups and *accuracy_score* (scikit-learn). Since the computer vision methods partly build on each other, images with inherited errors were manually excluded from further analysis to make quantitative statements about the functionality of the individual CV methods. For example, the length measurement depends on the detection of the mask R-CNN, which is why non-detected beaks were excluded from the length analysis. Images with non-detected peduncles were not excluded from the analysis, as these peduncles hardly influenced the length measurement due to their small size.

3. Results

3.1. Peduncles and beaks

The trained mask R-CNN model was used to recognize peduncles and beaks on bean pods in order to exclude these components from further analysis of length, caliber, and curvature. The network detected most peduncles correctly with an accuracy of 95.5% (Fig. 2a, c I–VI; supplement 4). 15 peduncles were missed (Fig. 2c VII–IX). In 3 cases, the network misclassified beaks as peduncles (Fig. 2c X,XI). Beaks were

a)

Computer Vision	Reference: No Peduncle	Reference: Peduncle	
No Peduncle	107	15	122 87.7%
Peduncle	3	274	277 98.9%
	110 97.3%	289 94.8%	399 95.5%

b)

Computer Vision	Reference: No Beak	Reference: Beak	
No Beak	5	17	22 22.7%
Beak	1	376	377 99.7%
	6 85.3%	393 95.7%	399 95.5%

c)

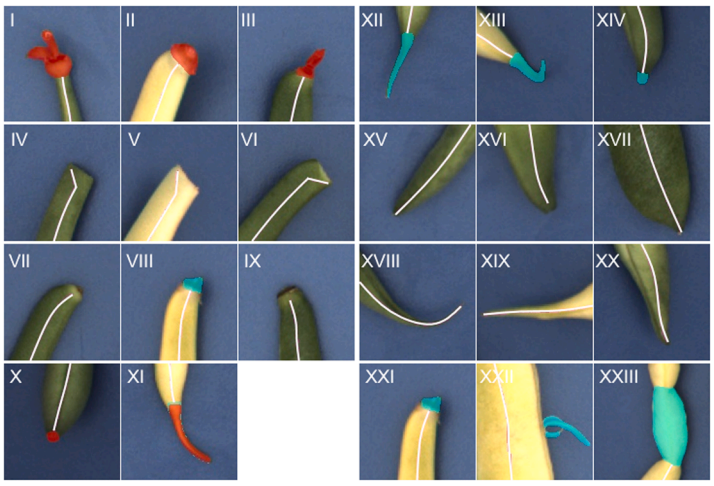

Fig. 2. Evaluation of the peduncle (a) and beak (b) classification: The reference values were acquired via visual scorings, the predictions were computed with a Mask R-CNN model. C) The model was capable to recognize very differently shaped peduncles and beaks (true positives in the top row peduncles I-III, beaks XII-XIV). Rarely, some pod ends were misclassified, e.g. true negatives in the second row (peduncles IV-VI, beaks XV-XVII), false negatives in the third row (peduncles VII-IX, beaks XVIII-XX) and false positives in the last row (peduncles X, XI, beaks XXI-XXIII). Red masks indicate peduncles and cyan masks indicate beaks as predicted by the Mask R-CNN.

detected with an accuracy of 95.5% (Fig. 2b, c XII–XVII), too. In 17 cases, the model was not able to detect the beak (Fig. 2c XVIII,XX). In two cases, 2 beaks were detected in a single bean pod (Fig. 2c XXI,XXII). In one case, the network predicted a beak in the center of the bean pod (Fig. 2c XXIII). This image was excluded from further analysis. The localization of both peduncles and beaks was very precise as indicated by a mAP50 of 92.3% for the validation data set during network training.

3.2. Length, caliber, and curvature

The computed pod lengths were well in linear accordance with the reference measurements conducted with a ruler (Fig. 3a, supplement 4). A total of 17 bean pods of 399 where the beak was not detected were excluded from the length analysis (Fig. 3a gray points). The regression shows a MAPE of 1.7% and a correlation coefficient of R=0.99 (Fig. 3a). To assess potential systematic size effects on the CV length analysis, residuals of the linear fit of three groups of bean pods were compared via One-Way ANOVA. The groups were divided according to Jusoh (2017) [5] into short (<120mm), medium (>=120mm, <=150mm), and long (>150mm). A p-value of 1 indicated no statistically significant differences between the length groups.

The caliber was computed from 399 single pod images and compared to the reference measurements that were taken with a circle drawing template (Fig. 3b, supplement 4). Bean pods which showed their narrow-curved side to the camera (6.6% of all bean pods, only pods from *Oval* and *Flat* categories) were excluded manually from the regression analysis. The linear fit displayed a MAPE of 3.3% and a correlation coefficient of R=0.99. Statistically significant differences were measured for the residuals of the regression between all bean pod categories (p=0.0008). The highest Cohen's D of 0.44 was measured for the residuals of the categories *Round* and *Flat* which still indicates a small effect size. This was also reflected by the residual plot which shows an even distribution around the zero line (supplement 5).

The CV estimations of the curvature were compared to the visual scorings performed according to breeder's standard (supplement 4). One feature of the breeder's rating scale was that it required a a more subtle gradation for lower curvatures (in our case the scoring classes 1-4), because new bean varieties are bred to be as straight as possible. The regression indicates a linear accordance between the computed log-transformed curvatures and the visual scores. A higher variation was observed for the scoring classes 1-4 (Fig. 3c). This was also reflected by a MAPE of 13.8% (R=0.81). A good agreement with the fit can also be observed when looking at the individual bean pod categories (Fig. 3c). No statistically significant differences were measured between residuals of the categories *Round, Oval*, and *Flat* (p=0.21). Only *Flat* bean pods of the scoring class 4 were underestimated slightly.

3.3. Seed arrangement

The seed formation in bean pods was assessed from images acquired with the backlight setup. In the yellow variety (Fig. 4a, b), the correct location of 93.3% of seeds and abortions was detected by the faster-RCNN (Fig. 4a). This result splits up into 96.9% correctly detected seeds and 76.7% correctly detected abortions. Pods with swan necks were detected in 90% of all cases (Fig. 4b). In comparison, the detection accuracy in the green variety (Fig. 4c, d) was only 79.8% in total, namely 82.9% for seeds and 42.9% for abortions (Fig. 4c). Swan necks were detected with an accuracy of 75.4% (Fig. 4d). Fig. 5 shows examples for successful (Fig. 5a-c) and non-successful (Fig. 5d) detection of seeds, abortions and swan necks.

3.4. Chromatic traits

Green bean pods were correctly separated from the yellow and bicolor bean pods via hue thresholding (100% accuracy). They were further analyzed with respect to the green brightness. The results show a clear linear relationship between the reference scores and computed green brightness values (Fig. 6, supplement 4). This was reflected by a MAPE of 2.1% and a high correlation (R=-0.87). Moreover, the residual analysis did not indicate statistically significant differences (p=0.39) between the bean pod categories *Round, Oval* and *Flat*. In the case of non-green pods, the RFC could distinguish between the yellow and the bicolor ones with a cross validation accuracy of 83 ±7% (n=10).

4. Discussion

The aim of this study was to develop computer vision methods for objective, reliable, repeatable, and fast evaluation of fruit quality traits. The results of the CV methods were compared to ratings of expert breeders for all traits examined, except for the analysis of the seed arrangement due to scoring uncertainties (as explained in 2.2). To quantify the performance of the methods presented in this manuscript, different measures of accuracy were calculated, including classification metrics, mean absolute percentage errors (MAPE), and correlation

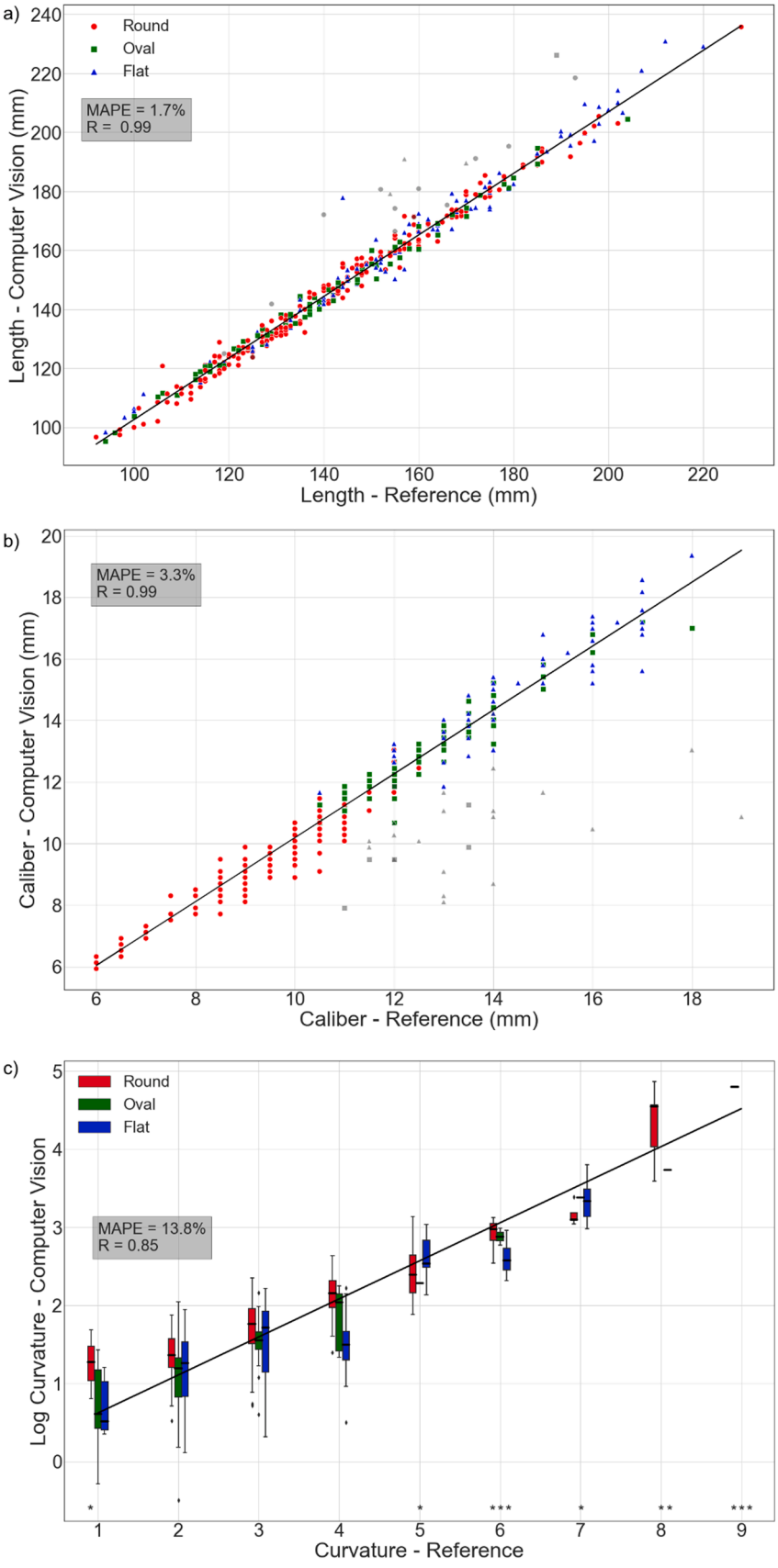

Fig. 3. Comparison of reference measurements/scores and CV estimations for different shape traits: a) Length, b) Caliber, and c) Curvature (n=399). The mean absolute percentage error (MAPE) and correlation coefficient R is plotted for all three traits. Outliers (grey) in a) indicate missed beak detections, n=17; while in b) bean pods of categories Oval and Flat that show their curved narrow side to the camera, (n=26) were not considered for the computation of the fit.. Stars in c) indicate boxplots with n<5.

a)

Computer Vision	Reference: Seed	Reference: Abortion	Reference: Not detected	
Seed	190	7		197 96.5%
Abortion	5	33		38 86.8%
Not detected	1	3		4 0.0%
	196 96.9%	43 76.7%	0 0.0%	239 93.3%

b)

Cumputer Vision	Reference: No swan neck	Reference: Swan neck	
No swan neck	9	4	13 69.2%
Swan neck	2	45	47 95.7%
	11 81.8%	49 91.8%	60 90.0%

c)

Computer Vision	Reference: Seed	Reference: Abortion	Reference: Not detected	
Seed	285			285 100.0%
Abortion	4	12		16 75.0%
Not detected	55	16		71 0.0%
	344 82.9%	28 42.9%	0 0.0%	372 79.8%

d)

Cumputer Vision	Reference: No swan neck	Reference: Swan neck	
No swan neck	40	9	49 81.6%
Swan neck	5	3	8 37.5%
	45 88.9%	12 25.0%	57 75.4%

Fig. 4. Performance evaluation for the CV estimations of different seed arrangement properties. The results from the Faster R-CNN predictions were compared to visual scorings for seeds and abortion occurrences in a) and c) and for swan necks in b) and d). These results are further broken down for the yellow (a, b, n=60) and the green variety (c, d, n=57). Accuracy, precision, and recall metrics are highlighted in green.

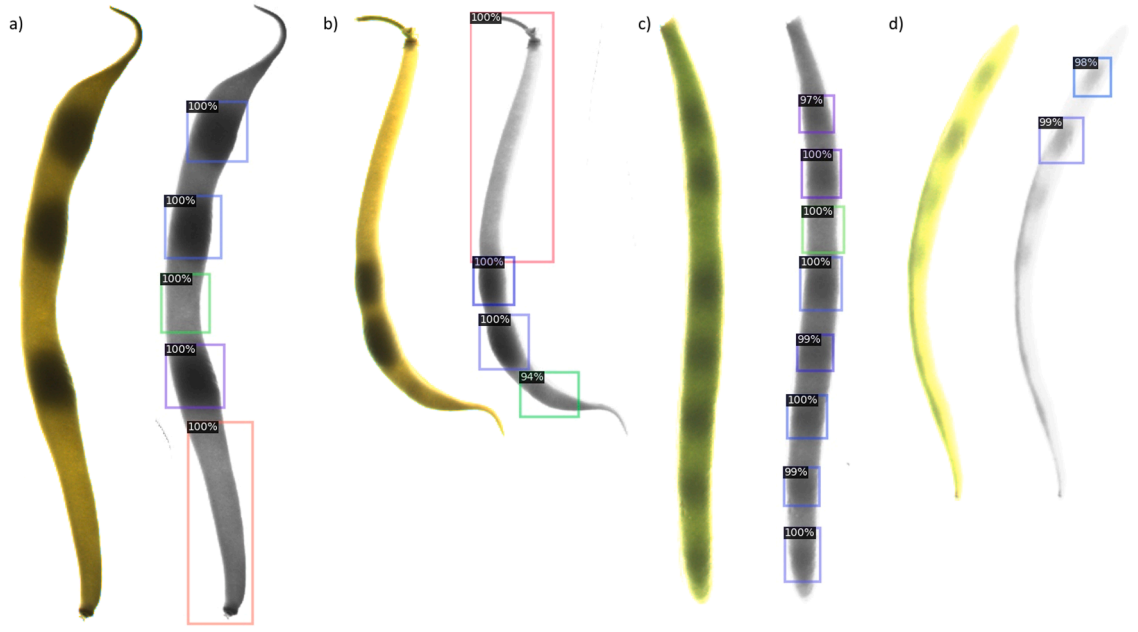

Fig. 5. Faster R-CNN predictions for seeds (blue rectangles), abortions (green rectangles), and swan necks (red rectangles). Values in the boxes indicate the confidence values. A) and b) display yellow bean pods, c) a darker green bean pod with bigger seeds, and d) a brighter green bean pod with smaller seeds

coefficients for regression analysis. In order to test the limits of the developed computer vision methods, a wide range of bean varieties with a large variation in the investigated traits was analyzed.

A customized imaging box enabled computer vision methods to accurately quantify bean pod characteristics: While imaging under field conditions was mainly used for fruit counting and pre-harvest yield assessment of beans [42,43], a fully controllable imaging box allows for precise evaluations of the traits of individual bean pods with a comparatively higher throughput than manual measurements. This applies in particular to the analysis of chromatic traits that require a constant color rendering, which is not given under field conditions. One challenge that arises from the imaging approach is the reduction of3D information using a 2D imaging setup, as bean pods can be analyzed from all sides during manual assessments.

Peduncles and beaks were detected and masked accurately, allowing precise analysis of further shape traits: For this study, the detection of peduncles is important in two ways. On the one hand, it provides information about the expected proportion of pods with or without peduncles and thus about harvest-relevant properties. The high detection rate of 94.8% allowed for a precise determination of peduncle occurrences (Fig. 2a). On the other hand, it is (together with the detection of the beaks) an important pre-processing step in order to take correct measurements on the pod. Although the second aspect was already studied in different crops/fruits by several groups [27,29,44], only one validated approach exists so far for bush bean pods that employed a combination of machine learning (RFC) and image processing [29]. We

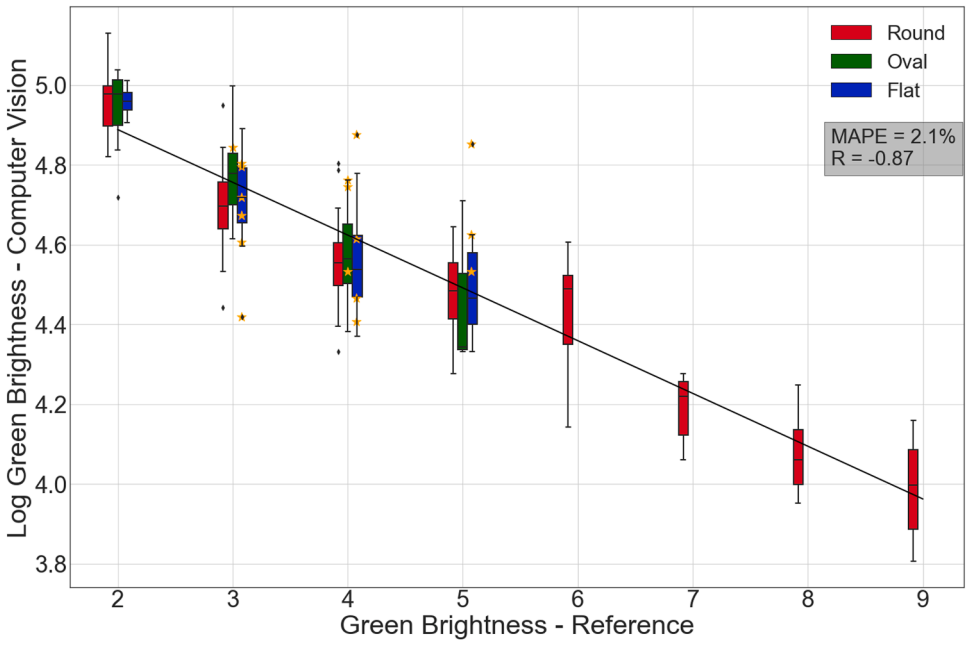

Fig. 6. Relationship between reference *scores for the green* brightness and log-transformed computer vision estimations. The orange-colored stars denote bean pods from the categories Oval and Flat which showed their narrow side towards the camera, while the visual assessment considered the broad side (n= 309).

tested this approach on our data and found that it did not reliably process images of all bean varieties. We assume that the methods were developed using data with less variation in some of the traits. In the field of deep learning, convolutional neural networks (CNN) have been successfully used for peduncle detection of bell peppers in the field [45]. We replaced the machine learning RFC approach (introduced in [29]) with a CNN model and were thus able to improve the detection accuracy despite the larger variation in data. Detected beaks and peduncles were masked very precisely, which was also reflected by accurate length estimations (Fig. 3a). In a few cases, the CNN missed peduncles mainly due to their size, i.e. no or barely any stem or petals were visible (Fig. 2c VII–IX), although it hardly affect the length estimation. In 4 pods, two beaks were detected. In these cases, a correct attribution could be made based on the confidence scores of the predictions.

Caliber measurement via CV was robust for the Round and slightly limited for the Flat and Oval pod categories: We showed a comprehensive validation of the caliber measurement method (Fig. 3b) reported in Jollet et al. (2021) [29]. Because we were able to improve the segmentation of bean pods, the caliber estimates are now more accurate, as reflected by a mean residual of 0.36mm (supplement 5). In case of 26 pods from the *Oval* and *Flat* category the caliber could not be measured accurately, because the pods showed their narrow side towards the camera. For automated estimations this could be overcome by comparing individual measurements to the median (as the mean is sensitive to outliers), as modern bean varieties used for breeding are quite uniform. The results of this study indicate that the main challenges arise from perspective issues. If the bean pod is strongly curved and flattened, the orientation towards the camera will determine the accuracy with which the curvature and caliber can be measured. This effect was perceived for the categories Oval and Flat, in particular.

Curvature can be estimated objectively and the CV method works robustly within the range of breeder scorings: A new method for calculating the curvature of a bean pod based on local derivatives was presented for the first time. It also takes into account a heterogeneous distribution of curvatures along the pod up to special shapes like S-shapes. This study represents a significant improvement compared to previous curvature measures based on the ratio of the minimum and maximum width of the convex hull of the center line [27] or the ratio of curved to straight length [46]. A curvature estimation based on local derivations was also conducted by Soleimanipour & Chegini (2019), who successfully measured the curvatures of cucumber contours using B-spline regression models [47]. In contrast to their approach, it was sufficient to approximate a single curved line, which is why we used less complex polynomial fitting functions. The perspective issues mentioned above are also evident in *Flat* bean pods of scored class 4. Some samples were positioned in a way that resulted in more accurate caliber than curvature measurements. There was one case, where 4 pods of a *Flat* variety displayed this peculiarity. Proper positioning of the bean pods, however will reduce this biasing effect. Furthermore, a relatively high MAPE was noticed for the curvature regression model. It should be noted that the MAPE metric is more sensitive to values close to 0, e.g. in the scoring classes 1-4. In addition, these deviations could also result from inaccuracies of the reference scoring. In our study, no twisted bean pods with a complex 3D curvature were present, as they are extremely rare and cannot be measured with a 2D imaging approach.

Seed arrangement analysis via backlight imaging is a promising approach: To conclude on the number of seeds, abortions, and swan neck, breeders rely on haptic assessment. The surface of the pod is typically gauged with fingers to count seeds and find abortions and swan necks. As such, there is a lack of visual feedback, which in turn can be problematic with small seeds or a missing seed marking as is the case with most breeding-relevant varieties. In this work, an approach to assess the seed arrangement of bean pods via transmitted light was presented. Since the haptic evaluation of the seed arrangement by the expert breeder differed substantially from the visual inspection of the backlight images, the latter was used as a reference Good results were obtained for the translucent yellow variety, where hardware setup and camera settings allowed us to achieve a good contrast between seeds and the rest of the pod. This facilitates further detection by the Faster R-CNN, a neural network model proven to be very efficient in various agricultural [48–50] and non-agricultural [51,52] contexts. On well-developed pods, seeds, abortions and swan necks were reliably identified by the faster R-CNN (Fig. 5a, b). The limitations of the approach were tested using a green variety with variable but comparatively low transmission, small seeds and pods at different stages of development. The results show that the accuracy of the CV method is mainly influenced by seed size and bean pod transmittance as a consequence of variety properties and age (Fig. 5c, d) and by the contrast between seeds and the rest of the pod.

The latter depends on the well-tuned settings of backlight illuminance and exposure time in relation to the pod transparency ranging between dark and bright (Fig. 5). In a sample set of mixed pod transparencies, good settings for dark pods resulted in overexposed bright pods (Fig. 5c, d) and vice versa. Further improvements could be achieved with a larger and more balanced training data set (regarding the number of green and yellow samples), which was not available for this study. On the hardware side, improvements could be achieved by employing a camera with a higher dynamic range or by acquiring a series of images with different backlight illuminances in combination with a contrast analysis of the pods to find the optimal illumination settings for each individual bean pod.

Bean color classification by hue thresholding and RF classification has proven to be an effective combination: A new method was presented not only to distinguish between green and yellow bean pods by hue thresholding, but also to identify rare bicolor pods, which are unwanted in breeding programs. Although limited data was available for this class, we were able to get sufficient results using an RFC model, which can help breeders identify yellow bean varieties that tend to produce bicolor pods.

Brightness of green bean pods can objectively be assessed with the presented CV system: With the CV approach, we were able to precisely measure the brightness of green bean pods. However, slight discrepancies between reference and CV measurements were observed for a few bean pods, which are featured by a different average brightness depending on which side is facing the camera. It is likely that in these cases, different pod sides were evaluated for reference and CV measurements.

Applicative value of the system in breeding programs: New plants can be assessed directly in the field with standard descriptors (e.g. according to UOPV guidelines), which is sufficient in the early steps of a breeding program for doing a first and not very stringent selection. During later steps in the program, the presented imaging system can help to find superior plants within the higher generations by testing the pod characteristics of the respective bulks (progenies of single plants). As modern varieties continue to converge, breeders seek for methods to find slightest differences in pod appearance, and the presented system provides a practical solution. Furthermore, the vegetable market sets specific requirements for the shape and color characteristics of bean pods. Are these requirements not fulfilled, a successful market entry is prevented even for a high-yielding variety. After imaging a set of different varieties (one image per variety with up to 40 pods per image), the software takes the images from a folder and processes each image and each pod one after the other and returns a .CSV file with the estimations for all traits in tandem with labeled image data for analysis back tracing. As the variety name is tracked during the whole process, the data can later be synchronized easily with other traits recorded during vegetation.

5. Conclusions

Evaluating quality traits of bush bean pods manually is a time-consuming process that generates a significant bottleneck in breeding programs. Currently, quality trait evaluations, which combine manual measurements and visual scorings, must be performed by experts; however, the reliability of this process remains susceptible to inter-rater variability and day-to-day variability for a given rater. The hardware setup and computer vision workflow presented in this study allows large amounts of samples to be analyzed with consistent repeatability. Various categories of bush bean pods were assessed with a throughput of approximately 45 pods per minute (run with *Geforce RTX 3070* graphics card). Therefore, the analysis software is much faster compared to the usual practice. The hardware setup could also be implemented in an assembly line for even higher throughput, helping to reduce the phenotyping bottleneck in bean breeding programs. In contrast to the visual assessment of curvature and brightness, the continuous scales allow for more distinct estimations. Although only green and yellow bean varieties were covered in this study, the methods for hue and brightness analysis could also be applied to violet or colorful spotted bean pods. An additional opportunity for extending the methodology presented in this work is seed coat pattern analysis, which could be made available by adding specific methods to the analysis software. For example a RF approach similar to the one of this study could be used to classify different properties of seed coats. Furthermore, we consider the backlight imaging method as a promising approach, which needs to be further developed to better analyze the properties of the seed arrangement.

Declaration of Competing Interest

The authors declare that they have no known competing financial interests or personal relationships that could have appeared to influence the work reported in this paper.

Data availability

The data that has been used is confidential.

Acknowledgments

This study was carried out as part of the ‘Shape & Color’ project, funded by the Ministry of economic affairs of Germany (IGF-Vorhaben 20943N) and supported by the *Gemeinschaft zur Förderung von Pflanzeninnovation e.V.* (GFPi). Special thanks to Van Waveren Saaten GmbH and its staff for supporting the study.

Supplementary materials

Supplementary material associated with this article can be found, in the online version, at doi:10.1016/j.atech.2023.100306.

References

[1] E. Sangronis, M. Rodríguez, R. Cava, A. Torres, Protein quality of germinated Phaseolus vulgaris, Eur. Food Res. Technol. 222 (2006) 144–148, https://doi.org/10.1007/s00217-005-0137-4.
[2] N. Petry, E. Boy, J.P. Wirth, R.F. Hurrell, Review: the potential of the common bean (icrosoft vulgaris) as a vehicle for iron biofortification, Nutrients 7 (2015) 1144–1173, https://doi.org/10.3390/nu7021144.
[3] R. King, K. Vining, Breeding snap beans for organic agriculture: genomic shifts under different agricultural management systems resistance and resistance breeding view project small fruits genetics view project, (2019). 10.13140/RG.2.2.12594.94408.
[4] C. Torres, A. Clément, E. Frison, E. Auperpin, P. Parmentier, A. Feutry, Image analysis for characterising French bean (Phaseolus vulgaris L.) Pods, 2012.
[5] M. Jusoh, The validation of QTL for pod quality and domestication traits through association mapping and genomics in snap beans, 2017.
[6] G. Latauschke, Mittelfeine buschbohnen bei sehr guten bedingungen mit spitzenerträgen, 2021.
[7] T. Ilakiya, E. Parameswari, V. Davamani, D. Swetha, E. Prakash, High-throughput crop phenotyping in vegetable crops, Pharma Innov. 9 (2020) 184–191, https://doi.org/10.22271/tpi.2020.v9.i8c.5035.
[8] I. Simko, R.J. Hayes, Accuracy, reliability, and timing of visual evaluations of decay in fresh-cut lettuce, PLOS One 13 (2018), https://doi.org/10.1371/journal.pone.0194635.
[9] M.A. Miller-Butler, B.J. Smith, K.J. Curry, E.K. Blythe, Evaluation of detached strawberry leaves for anthracnose disease severity using image analysis and visual ratings, HortScience 54 (2019) 2111–2117, https://doi.org/10.21273/HORTSCI14321-19.
[10] A. Chawade, J. van Ham, H. Blomquist, O. Bagge, E. Alexandersson, R. Ortiz, High-throughput field-phenotyping tools for plant breeding and precision agriculture, Agronomy 9 (2019), https://doi.org/10.3390/agronomy9050258.
[11] H. Tian, T. Wang, Y. Liu, X. Qiao, Y. Li, Computer vision technology in agricultural automation —a review, Inf. Process. Agric. 7 (2020) 1–19, https://doi.org/10.1016/j.inpa.2019.09.006.
[12] T. Yuan, C. Ji, Y. Chen, W. Li, J. Zhang, Greenhouse cucumber recognition based on spectral imaging technology, Trans. Chin. Soc. Agric. Mach. 42 (2011) 172–176.
[13] C.E. Yang, Spectral analysis and multispectral/hypersprectral imaging to detect blueberry fruit maturity stages for early blueberry yield estimation, 2013.

[14] H. Gan, W.S. Lee, V. Alchanatis, A. Abd-Elrahman, Active thermal imaging for immature citrus fruit detection, Biosyst. Eng. 198 (2020) 291–303, https://doi.org/10.1016/j.biosystemseng.2020.08.015.
[15] S.K. Gurupatham, N. Jacob, K. Van, D. Horn, F. Fahad, Fruit ripeness estimation for avocado using thermal imaging, 2018. https://proceedings.asmedigitalcollection.asme.org.
[16] J.Q. He, R.J. Harrison, B. Li, A novel 3D imaging system for strawberry phenotyping, Plant Methods 13 (2017) 93, https://doi.org/10.1186/s13007-017-0243-x.
[17] S.D. Turner, S.L. Ellison, D.A. Senalik, P.W. Simon, E.P. Spalding, N.D. Miller, An automated image analysis pipeline enables genetic studies of shoot and root morphology in carrot (daucus carota l, Front. Plant Sci. 871 (2018), https://doi.org/10.3389/fpls.2018.01703.
[18] M.H. Hu, Q.L. Dong, P.K. Malakar, B.L. Liu, G.K. Jaganathan, Determining banana size based on computer vision, Int. J. Food Prop. 18 (2015) 508–520, https://doi.org/10.1080/10942912.2013.833223.
[19] G. Bodner, M. Alsalem, A. Nakhforoosh, T. Arnold, D. Leitner, RGB and spectral root imaging for plant phenotyping and physiological research: Experimental setup and imaging protocols, J. Vis. Exp. (2017), https://doi.org/10.3791/56251, 2017.
[20] G. Lobet, X. Draye, C. Périlleux, An online database for plant image analysis software tools plant methods an online database for plant image analysis software tools, 2013. http://www.plantmethods.com/content/9/1/38http://www.plantmethods.com/content/9/1/38DATABASE.
[21] M.H. Malik, T. Zhang, H. Li, M. Zhang, S. Shabbir, A. Saeed, Mature tomato fruit detection algorithm based on improved HSV and watershed algorithm, Elsevier B. V. (2018) 431–436, https://doi.org/10.1016/j.ifacol.2018.08.183.
[22] K. Yamamoto, W. Guo, Y. Yoshioka, S. Ninomiya, On plant detection of intact tomato fruits using image analysis and machine learning methods, Sensors 14 (2014) 12191–12206, https://doi.org/10.3390/s140712191. Switzerland.
[23] A. Inur, A.F. Amri, A.R. Ismail, A.A. Zarir, Comparative performance of deep learning and machine learning algorithms on imbalanced handwritten data, 2018. www.ijacsa.thesai.org.
[24] K. He, G. Gkioxari, P. Dollár, R. Girshick, Mask R.C.N.N., (2017). http://arxiv.org/abs/1703.06870.
[25] M. Afonso, H. Fonteijn, F.S. Fiorentin, D. Lensink, M. Mooij, N. Faber, G. Polder, R. Wehrens, Tomato fruit detection and counting in greenhouses using deep learning, Front. Plant Sci. 11 (2020), https://doi.org/10.3389/fpls.2020.571299.
[26] M.T. Brewer, L. Lang, K. Fujimura, N. Dujmovic, S. Gray, E. van der Knaap, Development of a controlled vocabulary and software application to analyze fruit shape variation in tomato and other plant species, Plant Physiol. 141 (2006) 15–25, https://doi.org/10.1104/pp.106.077867.
[27] G. Polder, G. Blokker, G.W.A.M. van der Heijden, An ImageJ plugin for plant variety testing, 2012.
[28] N.D. Miller, N.J. Haase, J. Lee, S.M. Kaeppler, N. de Leon, E.P. Spalding, A robust, high-throughput method for computing maize ear, cob, and kernel attributes automatically from images, Plant J. 89 (2017) 169–178, https://doi.org/10.1111/tpj.13320.
[29] D. Jollet, U. Rascher, M. Müller-Linow, Assessing yield quality parameters in bush bean via RGB imagery, Acta Hortic. (2021).
[30] E.M. de Oliveira, D.S. Leme, B.H.G. Barbosa, M.P. Rodarte, R.G.F.A. Pereira, A computer vision system for coffee beans classification based on computational intelligence techniques, J. Food Eng. 171 (2016) 22–27, https://doi.org/10.1016/j.jfoodeng.2015.10.009.
[31] Z. Zhang, A flexible new technique for camera calibration, 1998. http://research.microsoft.com/~zhanghttp://research.microsoft.com/~zhang.
[32] G. van Rossum, F.L. Drake, Python 3 Reference Manual, Scotts Vallay, CA, 2009.
[33] C.R. Harris, K.J. Millman, S.J. van der Walt, R. Gommers, P. Virtanen, D. Cournapeau, E. Wieser, J. Taylor, S. Berg, N.J. Smith, R. Kern, M. Picus, S. Hoyer, M.H. van Kerkwijk, M. Brett, A. Haldane, J.F. del Río, M. Wiebe, P. Peterson, P. Gérard-Marchant, K. Sheppard, T. Reddy, W. Weckesser, H. Abbasi, C. Gohlke, T.E. Oliphant, Array programming with NumPy, Nature 585 (2020) 357–362, https://doi.org/10.1038/s41586-020-2649-2.
[34] G. Bradski, The OpenCV Library, Dr. Dobb's Journal of Software Tools. (2000).
[35] F. Pedregosa, G. Varoquaux, A. Gramfort, V. Michel, B. Thirion, O. Grisel, M. Blondel, P. Prettenhofer, R. Weiss, V. Dubourg, J. Vanderplas, A. Passos, D. Cournapeau, M. Brucher, M. Perrot, É. Duchesnay, Scikit-learn: machine learning in python, J. Mach. Learn Res. 12 (2011) 2825–2830. http://scikit-learn.sourceforge.net.
[36] Y. Wu, A. Kirillov, F. Massa, W.Y. Lo, R. Girshick, Detectron2, (2019). https://github.com/facebookresearch/detectron2 (accessed June 9, 2022).
[37] Meta Research, Detectron2 – model zoo, https://Github.Com/Facebookresearch/Detectron2/Blob/Main/MODEL_ZOO.Md. (2022).
[38] A. Dutta, A. Zisserman, The VIA Annotation Software for Images, Audio and Video, n.d. http://www.robots.ox.ac.uk/.
[39] A. Vadivel, S. Sural, A.K. Majumdar, Human color perception in the HSV space and its application in histogram generation for image retrieval. Color Imaging X: Processing, Hardcopy, and Applications, SPIE, 2005, p. 598, https://doi.org/10.1117/12.586823.
[40] A.R. Smith, Color Gamut Transform Pairs, IEEE Computer Society Press, 1978, pp. 376–383.
[41] J. Cohen, Statistical Power Analysis for the Behavioral Sciences, 2nd ed., Lawrence Erlbaum Accociates, 1988.
[42] W. Lu, R. Du, P. Niu, G. Xing, H. Luo, Y. Deng, L. Shu, Soybean yield preharvest prediction based on bean pods and leaves image recognition using deep learning neural network combined With GRNN, Front. Plant Sci. 12 (2022), https://doi.org/10.3389/fpls.2021.791256.
[43] U.F. Rahim, T. Utsumi, H. Mineno, Deep learning-based accurate grapevine inflorescence and flower quantification in unstructured vineyard images acquired using a mobile sensing platform, Comput. Electron. Agric. 198 (2022), 107088, https://doi.org/10.1016/j.compag.2022.107088.
[44] S. Cubero, M.P. Diago, J. Blasco, J. Tardáguila, B. Millán, N. Aleixos, A new method for pedicel/peduncle detection and size assessment of grapevine berries and other fruits by image analysis, Biosyst. Eng. 117 (2014) 62–72, https://doi.org/10.1016/j.biosystemseng.2013.06.007.
[45] C. Lehnert, C. McCool, T. Perez, In-field peduncle detection of sweet peppers for robotic harvesting: a comparative study, (2017). http://arxiv.org/abs/1709.10275.
[46] S. Haque, E. Lobaton, N. Nelson, C. Yencho, Computer vision approach to characterize size and shape phenotypes of horticultural crops using high-throughput imagery, Comput. Electron. Agric. 182 (2021), https://doi.org/10.1016/j.compag.2021.106011.
[47] A. Soleimanipour, G.R. Chegini, Three-dimensional reconstruction of cucumbers using a 2D computer vision system, J. Food Meas. Charact. 13 (2019) 571–578, https://doi.org/10.1007/s11694-018-9970-6.
[48] L. Fu, Y. Feng, Y. Majeed, X. Zhang, J. Zhang, M. Karkee, Q. Zhang, Kiwifruit detection in field images using faster R-CNN with ZFNet, IFAC Pap. 51 (2018) 45–50, https://doi.org/10.1016/j.ifacol.2018.08.059.
[49] Z. Li, Y. Li, Y. Yang, R. Guo, J. Yang, J. Yue, Y. Wang, A high-precision detection method of hydroponic lettuce seedlings status based on improved faster RCNN, Comput. Electron. Agric. 182 (2021), 106054, https://doi.org/10.1016/j.compag.2021.106054.
[50] Q. Wang, F. Qi, Tomato Diseases Recognition Based on Faster RCNN, in: Proceedings of the 10th International Conference on Information Technology in Medicine and Education (ITME), IEEE, 2019, pp. 772–776, https://doi.org/10.1109/ITME.2019.00176.
[51] Y. Kawazoe, K. Shimamoto, R. Yamaguchi, Y. Shintani-Domoto, H. Uozaki, M. Fukayama, K. Ohe, Faster R-CNN-based glomerular detection in multistained human whole slide images, J. Imaging 4 (2018), https://doi.org/10.3390/jimaging4070091.
[52] V.K. Mishra, S. Bhowmick, S. Saleem, Agriculture Field Security System Using Faster R-CNN, in: 2022: pp. 464–471. 10.1007/978-981-19-1742-4_39.